

Atomic-scale surface demixing in a eutectic liquid BiSn alloy

Oleg G. Shpyrko,^{1,*} Alexei Yu. Grigoriev,^{1,†} Reinhard Streitel,¹
Diego Pontoni,¹ Peter S. Pershan,¹ Moshe Deutsch,² and Ben Ocko³

¹*Department of Physics and DEAS, Harvard University, Cambridge MA 02138*

²*Department of Physics, Bar-Ilan University, Ramat-Gan 52900, Israel*

³*Department of Physics, Brookhaven National Laboratory, Upton NY 11973*

(Dated: January 27, 2020)

Resonant x-ray reflectivity off a liquid eutectic Bi₄₃Sn₅₇ alloy's surface reveals atomic-scale demixing extending over three near-surface atomic layers. The near-complete Bi segregation in the topmost monolayer agrees well with the Gibbs adsorption theorem. However, the Bi depletion in the second, and small enhancement in the third, monolayers are not predicted by the Gibbs theory. The Prigogine-Defay adsorption theory is shown to account for the observed compositional modulations, revealing a near-surface domination of the attractive Bi-Sn interaction over the entropy.

PACS numbers: 68.10.-m, 61.10.-i

The widely-accepted Gibbs adsorption rule [1] predicts the surface segregation of the lower surface energy component of a binary mixture. Liquid metals are ideal systems for studying Gibbs adsorption due to the nearly spherical shape of interacting particles, relative simplicity of the short-range interactions and the availability of bulk thermodynamic data for many binary alloys. While certain aspects of Gibbs theory can be tested through macroscopic measurement of surface tension or adsorption isotherms, there have been very few direct measurements of the atomic-scale composition profiles of the liquid-vapor interface [2, 3, 4]. In addition to fundamental questions related to surface thermodynamics of binary liquids, BiSn-based alloys have been widely studied as substitutes for toxic Pb-based low-melting solders [5]. Thus, understanding their wetting, spreading, alloying, reactivity and other surface-related properties are of great practical importance. Moreover, interfacial phenomena dominate the properties of the increasingly important class of nanoscale materials, as demonstrated recently in studies of the liquid-solid phase stability of nanometer-sized BiSn particles [6].

Synchrotron-based x-ray reflectivity (XR) techniques now allow the determination of the surface-normal density profile of a liquid with Ångström-scale resolution. Over the last few years these techniques revealed the long-predicted surface-induced atomic layering at the liquid-vapor interface for a number of elemental liquid metals [7, 8, 9, 10, 11]. *Resonant* x-ray reflectivity near an absorption edge resolved the density profile of each component in GaIn [2], HgAu [3] and BiIn [4] liquid binary alloys. The enhancement of the concentration of the low-surface tension component was invariably found to be confined to the topmost surface monolayer, with subsequent layers having the composition of the bulk, in accord with the simplest interpretation of the Gibbs rule. By contrast, the present study reveals an atomic-scale phase separation extending over at least three atomic layers. These results are somewhat unexpected, considering

the eutectic nature, and nearly perfect solution behavior, of the Bi₄₃Sn₅₇ alloy.

A liquid Bi₄₃Sn₅₇ sample (99.99% purity, Alfa Aesar) was prepared under UHV conditions ($P < 10^{-9}$ Torr). Atomically clean liquid surfaces were prepared by mechanical scraping and Ar⁺ ion sputtering, as described previously [10, 12, 13]. Measurements were done at the liquid surface diffractometer, ChemMatCARS beamline, Advanced Photon Source, Argonne National Laboratory at a sample temperature of $T = 142$ °C, 4 °C above the Bi₄₃Sn₅₇ alloy's eutectic temperature, $T_e = 138$ °C.

The reflected intensity fraction, $R(q_z)$, of an x-ray beam impinging on a structured liquid surface at a grazing angle α , is given within the kinematic Born approximation by:

$$R(q_z) = R_F(q_z) \cdot |\Phi(q_z)|^2 \cdot CW(q_z) \quad (1)$$

where $q_z = (4\pi/\lambda) \sin \alpha$, λ is the wavelength of the x-rays, $R_F(q_z)$ is the Fresnel XR of an ideally abrupt and flat surface, $CW(q_z)$ is due to thermal surface capillary waves [9, 10], and the conventional (complex) structure factor of the interface, $\Phi(q_z)$, is given by [14]:

$$\Phi(q_z) = \frac{1}{\rho_\infty} \int dz \frac{d\langle \rho(z) \rangle}{dz} \exp(iq_z z) \quad (2)$$

where z is the surface-normal direction, ρ_∞ and $\rho(z)$ are the bulk and surface electron densities, respectively, and $\langle \dots \rangle$ denotes averaging over the surface-parallel directions. As R_F is a universal function depending only on the known critical angle for total external reflection, and $CW(q_z)$ is known accurately from capillary wave theory, the intrinsic density profile, $\langle \rho(z) \rangle$, is extracted from the measured $R(q_z)$ by computer fitting a physically motivated model, which we now describe [10].

The (forward) atomic scattering factor of a Z -electron atom varies with energy as [14]: $Z' = Z + f'(E) - if''(E)$, where $f'(E)$ and $f''(E) = \mu(E)\lambda/(4\pi)$, are the real and imaginary parts of the dispersion correction, and $\mu(E)$ is the photoelectric absorption coefficient.

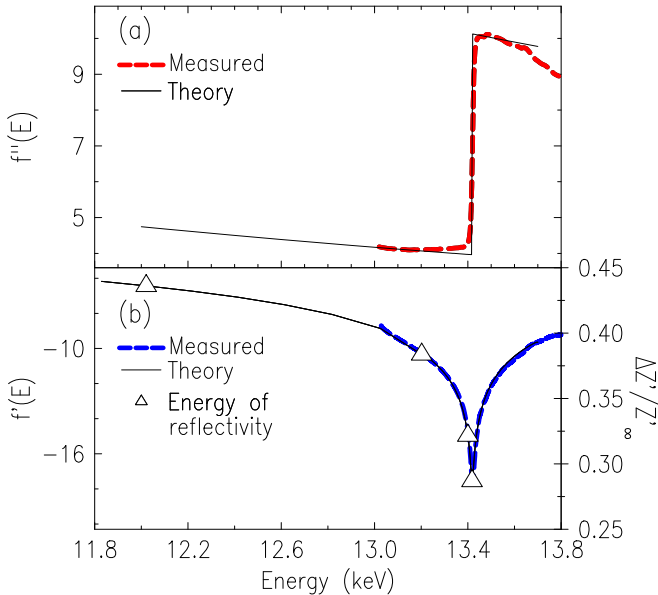


FIG. 1: Dispersion corrections (a) $f'(E)$ and (b) $f''(E)$ of Bi near the L3 absorption edge at $E_K = 13.418$ keV. Right scale of the lower graph represents electron density contrast $\Delta Z'/Z'_\infty = (Z'_\text{Bi} - Z'_\text{Sn})/Z'_\infty$.

The effect of f'' on the analysis can be neglected and the changes in f' are significant only near an absorption edge. Fig. 1(a) shows $f''(E)$ near the Bi L3 edge as obtained from an absorption measurement in a Bi foil. Fig. 1(b) shows the corresponding $f''(E)$ as calculated from the measured $f''(E)$ by numerical integration of the Kramers-Kronig relation [15]. Both agree well with theory [16, 17]. The composition dependence of $\langle \rho(z) \rangle$ was obtained by fitting the measured reflectivity with the distorted crystal (DC) model for a layered liquid surface [7, 8]:

$$\frac{\langle \rho(z) \rangle}{\rho_\infty} = \sum_{n=1}^{\infty} \frac{e^{-(z-nd)^2/\sigma_n^2}}{\sqrt{2\pi}\sigma_n/d} \left(1 + \delta_n \frac{Z'_\text{Bi} - Z'_\text{Sn}}{Z'_\infty}\right) \frac{c_n}{c} \quad (3)$$

The progressive increase in the Gaussian width parameter $\sigma_n^2 = \sigma_0^2 + (n-1)\bar{\sigma}^2$ with increasing layer number n is a convenient way of describing the decay in the amplitude of the layering away from the surface [8]. The layer spacing d is kept constant in this model due to similarity in size between Bi and Sn atoms, while $Z'_\infty = xZ'_\text{Bi} + (1-x)Z'_\text{Sn}$ is the average effective electron number per atom in the bulk, and $\delta_n = x'_n - x$ is the difference between the Bi fraction in the n -th layer, x'_n , in the bulk, x . The corresponding atomic densities, c_n and c , are determined from the atomic volumes v_Bi and v_Sn : $c_n x'_n v_\text{Bi} + c_n (1-x'_n) v_\text{Sn} = 1$. The contrast, $(Z'_\text{Bi} - Z'_\text{Sn})/Z'_\infty$, varies strongly near the edge due to the variation of Z'_Bi : from 0.43 at $E=12.00$ keV to 0.27 at $E=13.418$ keV (right axis in Fig. 1). This is the basis for the resonant x-ray reflectivity technique, which allows to

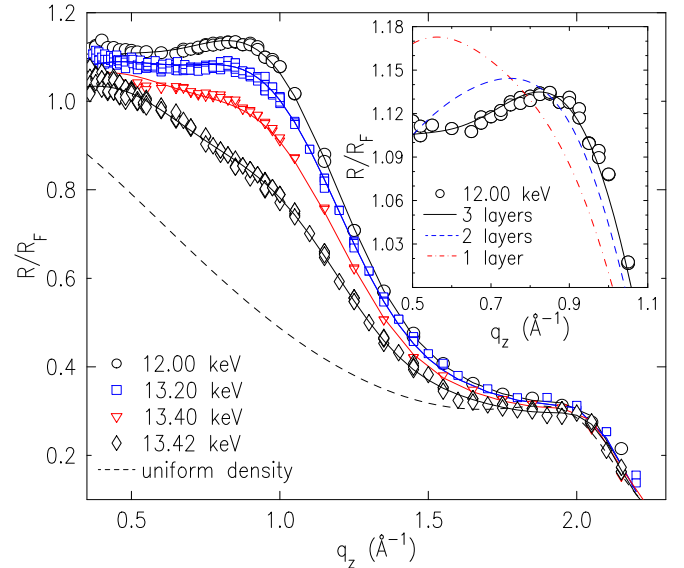


FIG. 2: X-ray reflectivities measured at the indicated energies, with fits by the three-layer model (lines). The dashed line is reflectivity assuming uniform composition in all atomic layers. Inset: The $E=12.00$ keV measured R/R_F with fits by the three models discussed in the text (lines). Error bars are smaller than the symbols' size.

separate out the density profiles of the two species. Further details are given in Refs. 4, 13.

Fig. 2 shows Fresnel-normalized reflectivities $R(q_z)/R_F(q_z)$ measured in the vicinity of the Bi L3 edge at the four energies marked by triangles in Fig. 1(b). The dashed line is $R(q_z)/R_F(q_z)$ calculated from the DC model for a layered interface with a *uniform* composition ($\delta_n = 0$). The strong enhancement of the measured $R(q_z)/R_F(q_z)$ over this line, evidenced by the peak at $q_z \simeq 1.0 \text{ \AA}^{-1}$, and the strong energy-dependence of the low- q_z reflectivity, clearly indicate a significant surface segregation of Bi, and its variation with z .

Three fits of the data by the DC model of Eq. 3 were carried out, assuming that only one ($\delta_1 \neq 0$, $\delta_{n \geq 2} = 0$), two ($\delta_{1,2} \neq 0$, $\delta_{n \geq 3} = 0$), or three ($\delta_{1,2,3} \neq 0$, $\delta_{n \geq 4} = 0$) surface layers deviate from the bulk composition. All fits employed $d = 2.90 \text{ \AA}$, $\sigma_0 = 0.30 \text{ \AA}$ and $\bar{\sigma} = 0.57 \text{ \AA}$, derived from the energy-independent position, shape and intensity of the layering peak at $q_z = 2.0 \text{ \AA}^{-1}$. The measured $R(q_z)/R_F(q_z)$ of all four energies were fitted simultaneously, using the experimentally determined $f'(E)$. As shown in Fig. 2 the three-layer model (solid lines) agrees with the data extremely well, while the inset shows that the one- and two-layer models do not. Table I lists the x'_n and $\delta_n^{Fit} = x'_n - x$ values obtained from the best fit, and the corresponding 95% non-linear confidence intervals $Y(x'_n)$ and $Y(\delta_n^{Fit})$ determined from a six-parameter support plane analysis [18]. The most striking result is the non-monotonic deviation δ_n of Bi from the 43% bulk value, showing an enhancement of 53% and 10% in the

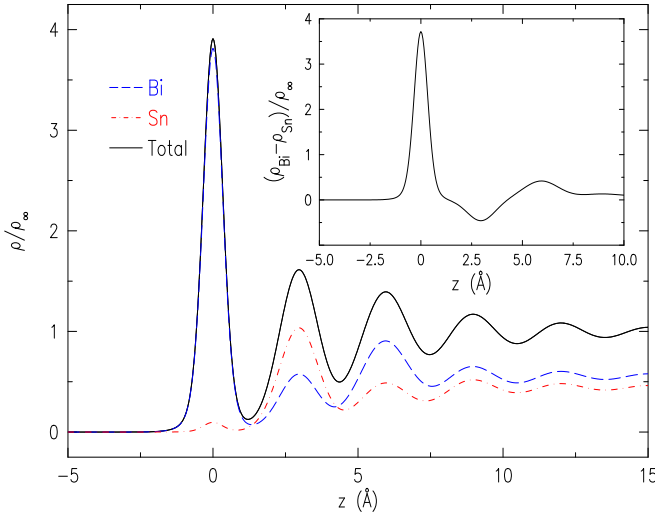


FIG. 3: Electron density profiles as derived from the fits to the reflectivities shown in Fig. 2. Inset: the bulk-normalized differences in electron density of Bi and Sn, $(\rho_{Bi} - \rho_{Sn})/\rho_{\infty}$.

first and third layers, and a depletion of 18% in the second layer. These effects are clearly observed in the atom-resolved density profiles obtained from the fits, shown in Fig. 3. Beyond the third layer entropy effects dominate the Gibbs adsorption and there is no detectable difference between the layer and bulk concentrations. We now compare these experimental observations with theory.

The Gibbs theory [1] of perfect binary solutions, and its extension to regular solutions [19], assume the surface segregation to be restricted to a single surface monolayer. A layered lattice model, that is appropriate for our layered liquid metal surface, is employed where the number of nearest neighbors of each atom within the monolayer is lp and in the next layer - mp . Here p is the total number of nearest neighbors of an atom in the bulk. For a close-packed lattice, for example, $p = 12$, $l = 0.5$ and $m = 0.25$. The surface tension of the regular solution, γ_{AB} , follows from those of the pure components, γ_A and γ_B , as [19]:

$$\begin{aligned} \gamma_{AB} &= \gamma_B + \frac{kT}{a_B} \ln\left(\frac{1-x'}{1-x}\right) + \frac{\omega}{a_B} [lx'^2 - (l+m)x^2] \quad (4) \\ &= \gamma_A + \frac{kT}{a_A} \ln\left(\frac{x'}{x}\right) + \frac{\omega}{a_A} [l(1-x')^2 - (l+m)(1-x)^2]. \end{aligned}$$

Here, x and $(1-x)$ are the bulk concentrations of atoms A (Bi) and B (Sn), while $x' \neq x$ and $(1-x')$ are the corresponding surface concentrations, a_A and a_B are the two atomic areas, and $\omega = 2\omega_{AB} - \omega_{AA} - \omega_{BB}$ is the interaction parameter, defined by the A-B, A-A and B-B atomic interaction energies. Extrapolated down to $T = 142$ °C, $\gamma_{Bi} = 398$ mN/m and $\gamma_{Sn} = 567$ mN/m, while a_{Bi} and a_{Sn} are calculated from the atomic radii $r_{Bi} = 1.70$ Å and $r_{Sn} = 1.62$ Å assuming hexagonally close packing [20]. Treating $Bi_{43}Sn_{57}$ as a perfect solution ($\omega/kT = 0$),

n	$x'_n(\text{Bi})$	$Y(x'_n)$	δ_n^{Fit}	$Y(\delta_n^{Fit})$	δ_n^{Theory}
1	0.96	[0.94, 0.99]	0.53	[0.51, 0.56]	0.47
2	0.25	[0.18, 0.27]	-0.18	[-0.25, -0.16]	-0.23
3	0.53	[0.50, 0.56]	0.10	[0.07, 0.13]	0.12
4	0.43	-	0	-	-0.06

TABLE I: density model parameters x'_n and $\delta_n^{Fit} = x'_n - x$ along with confidence intervals $Y(x'_n)$ and $Y(\delta_n^{Fit})$ obtained from least-squared fit to the three-layer model compared to theoretical δ_n^{Theory} derived from Gibbs theorem ($n=1$) and the extended Defay-Prigogine model ($n=2, 3, 4$).

the Gibbs theorem, Eq. 4, yields $\gamma_{AB} = 444$ mN/m and $x' = 0.904$, below the experimental value $x'_1(\text{Bi})$ in Table I. However, assuming a regular solution behavior with $\omega/kT = 1$ yields $\gamma_{AB} = 432$ mN/m, and $x' = 0.941$, which agrees very well with the experimentally derived $x'_1(\text{Bi})$ in Table I. Both γ_{AB} agree well with experiment and theory [21]. The relatively weak dependence of the Bi surface excess on the interaction parameter ω/kT should not be too surprising, since the excess also depends on the surface tension difference of the two components, $a_{Sn}\gamma_{Sn} - a_{Bi}\gamma_{Bi} \approx 2 kT$.

In spite of the good agreement above, the assumption of a monolayer-confined excess is correct for perfect solutions only, but not for our case of a regular solution. This was pointed out by Defay and Prigogine [22]. They provide a correction for regular solutions, where the surface excess extends over two layers, without significantly changing the γ_{AB} values obtained above. The corrected excess values are related by:

$$\ln \frac{1 + \delta_2/x}{1 - \delta_2/(1-x)} - \frac{2\omega}{kT} \delta_2 - \frac{2\omega m}{kT} (\delta_1 - 2\delta_2) = 0. \quad (5)$$

Assuming $|\delta_2| \ll 1$, and expanding Eq. 5 to first order in δ_2 :

$$\delta_2 = \frac{2\omega mx(1-x)\delta_1}{kT - 2\omega lx(1-x)}. \quad (6)$$

For nearly perfect solutions ($\omega/kT \ll 1$) Eq. 5 results in negligibly small δ_2 : $0 < \delta_2 \ll \delta_1$. For sufficiently large ω/kT , however, δ_2 and δ_1 are of opposite signs and $|\delta_2|$ may become comparable to $|\delta_1|$. This prediction is qualitatively consistent with the demixing observed in this study. For example, when $\omega/kT \gg 1$, Eq. 6 can be simplified further: $\delta_2 = -(m/l)\delta_1$. For $Bi_{43}Sn_{57}$, $m/l \approx 0.5$ and the Gibbs-predicted $x'_1 = 0.90$ (or $\delta_1 = 0.47$) yields $\delta_2 = -0.23$, $\delta_3 = 0.12$ and $\delta_4 = -0.06$ [23]. These values, shown as δ_n^{Theory} in Table I, agree well with δ_n^{Fit} obtained from the three-layer model fits. The smallest value of the interaction parameter ω/kT for which satisfactory agreement with the Defay-Prigogine model could be obtained (by treating m as an adjustable parameter) is $\omega/kT = 2.3$ for $m \ll l$, and is in good agreement with the $\omega/kT \approx 2.3$ demixing limit found in surface frozen

layers in alkane and alcohol binary mixtures [24], a system with very different interactions.

Theoretically, ω is related directly to the enthalpy of mixing, ΔH_m , through $\omega = \Delta H_m/[x(1-x)]$. In practice, however, bulk thermodynamic quantities were often found to yield inaccurate values for surface quantities. For example, reviews of Gibbs adsorption in organic [25] and metallic [26] mixtures point out significant disagreements between ω values empirically derived from surface tension measurements and those calculated from bulk calorimetry. The reported values of ΔH_m range from endothermic values of 80 to 140 J/mol [27] to an exothermic value of -180 J/mol [28]. These values lead to $|\omega/kT| < 0.2$, i.e. an almost perfect solution, and an insignificant $|\delta_2| < 0.01$. On the other hand, the value of $\omega/kT \approx 10$ that we previously found necessary to account for the observed 35% Bi concentration enhancement at the surface monolayer at the BiIn eutectic is of the same order of magnitude as the value we find necessary to account for the present observation of surface segregation in BiSn, $\omega/kT \approx 2.3$. In fact, the lattice model accounts well for the directly observed composition modulation in the near-surface layer of BiSn only when $\omega \gg kT$. Unfortunately we do not have an explanation for the origin of the discrepancy in the values of ω/kT and this suggests an urgent need for both further theoretical studies of surface demixing as well as experimental investigations of similar effects in other binary alloys. In particular, the BiSn system appears to be the only alloy for which clear evidence for multilayer surface demixing has been found. The case for new studies is strongly reinforced by the existence of a growing class of surface-induced ordering phenomena that have been observed in metallic liquids. In addition to the surface demixing reported here, these include layering [7, 8, 9, 10, 11], relaxation [11], segregation [2, 3, 4, 29], wetting transitions [12, 30], and surface freezing [31]. Finally, there is a basic unresolved question of whether the surfaces of liquid metals are fundamentally different from those of non-metallic liquids [32].

This work has been supported by the U.S. DOE grants No. DE-FG02-88-ER45379, DE-AC02-98CH10886 and the U.S.-Israel Binational Science Foundation, Jerusalem. We gratefully acknowledge useful discussions with E. Sloutskin at Bar-Ilan as well as assistance from B. Lin, T. Gruber, M. Meron and J. Gebhardt at ChemMat-CARS Sector 15, principally supported by the NSF/DOE grant No. CHE0087817. The Advanced Photon Source is supported by the U.S. DOE contract No. W-31-109-Eng-38.

[†] present address: University of Wisconsin-Madison, Madison, WI, 53706

- [1] J. W. Gibbs, R. G. V. Name, W. R. Longley and H. A. Bumstead, *The collected works of J. Willard Gibbs* (Longmans, New York, 1928).
- [2] M. J. Regan *et al.*, Phys. Rev. B **55**, 15874 (1997).
- [3] E. DiMasi *et al.*, MRS Symposium Series **590**, 183 (2000).
- [4] E. DiMasi *et al.*, Phys. Rev. Lett. **86**, 1538 (2001).
- [5] K. N. Tu *et al.*, J. Appl. Phys. **93**, 1335 (2003); J. Glazer, Int. Mat. Rev. **40**, 65 (1995).
- [6] J. G. Lee and H. Mori, Phys. Rev. B **70**, 144105 (2004).
- [7] O. M. Magnussen *et al.*, Phys. Rev. Lett. **74**, 4444 (1995).
- [8] M. J. Regan *et al.*, Phys. Rev. Lett. **75**, 2498 (1995).
- [9] H. Tostmann *et al.*, Phys. Rev. B **59**, 783 (1999).
- [10] O. G. Shpyrko *et al.*, Phys. Rev. B **67**, 115405 (2003).
- [11] O. G. Shpyrko *et al.*, Phys. Rev. B **70**, 224206 (2004).
- [12] P. Huber *et al.*, Phys. Rev. Lett. **89**, 035502 (2002).
- [13] O. G. Shpyrko, Ph.D. thesis, Harvard University, 2003 (unpublished).
- [14] J. Als-Nielsen and D. McMorrow, *Elements of Modern X-ray Physics* (Wiley, New York, 2001).
- [15] G. Evans and R. F. Pettifer, J. Appl. Cryst. **34**, 82 (2001); J. J. Hoyt *et. al.*, J. Appl. Cryst. **17**, 344 (1984).
- [16] E. A. Merritt, Anomalous Scattering Coefficients, <http://www.bmsc.washington.edu/scatter/> (1996-2003).
- [17] M. Newville, computer code IFEFFIT, (1997-2004).
- [18] P. R. Bevington and D. K. Robinson, *Data Reduction and Error Analysis for the Physical Sciences* (McGraw-Hill, New York, 1992) p. 212.
- [19] E. A. Guggenheim, Trans. Faraday Soc. **41**, 150 (1945).
- [20] CRC Handbook of Chemistry and Physics, ed. by D. R. Lide (CRC, Boca Raton, 1996).
- [21] S. W. Yoon *et al.*, Script. Mat. **40**, 297 (1999).
- [22] R. Defay and I. Prigogine, Trans. Faraday Soc. **46**, 199 (1950); R. Defay and I. Prigogine, *Surface Tension and Adsorption* (Wiley, New York, 1966).
- [23] Eq. 6 yields δ_3 from δ_2 and δ_4 from δ_3 .
- [24] E. Sloutskin *et al.*, Phys. Rev. B **68**, 031606 (2003).
- [25] G. L. Gaines, Trans. Faraday Soc. **65**, 2320 (1969).
- [26] T. P. Hoar and D. A. Melford, Trans. Faraday Soc. **53**, 315 (1957).
- [27] N. A. Asryan and A. Mikula, Inorg. Mat. **40**, 386 (2004); R. Hultgren *et al.*, *Selected Values of the Thermodynamic Properties of Binary Alloys* (Metals Park, OH, 1973); R. L. Sharkey and M. J. Pool, Metall. Trans. **3**, 1773 (1972); H. Seltz *et al.*, J. Am. Chem. Soc. **64**, 1392 (1942).
- [28] S. A. Cho and J. L. Ochoa, Metall. Mater. Trans. B **28**, 1081 (1997).
- [29] E. B. Flom *et al.*, Science **260**, 332 (1993).
- [30] H. Shim *et al.*, Surf. Sci. **476**, L273 (2001); A. H. Ayyad and W. Freyland, *ibid.* **506**, 1 (2002).
- [31] A. Issanin *et al.*, J. Chem. Phys. **121**, 12005 (2004); B. Yang *et al.*, Phys. Rev. B **62**, 13111 (2000); O. G. Shpyrko *et al.*, in preparation (2005).
- [32] E. Chacón and P. Tarazona, Phys. Rev. Lett. **91**, 166103 (2003); D. X. Li and S. A. Rice, J. Phys. Chem. B **108**, 19640 (2004); O. G. Shpyrko *et al.*, Phys. Rev. B **69**, 245423 (2004).

* Electronic address: oleg@xray.harvard.edu; present address: Center for Nanoscale Materials, Argonne National Laboratory, Argonne, IL, 60439